Theoretical study of solitonlike propagation of picosecond light pulses interacting with Wannier excitons

I. Talanina, D. Burak, R. Binder, H. Giessen,* and N. Peyghambarian
Optical Sciences Center, University of Arizona, Tucson, Arizona 85721
(Received 2 June 1997; revised manuscript received 4 February 1998)

An analytical and numerical study of light pulse propagation in semiconductors, with pulses spectrally centered at the lowest exciton resonance, is presented. It is shown that, in the limit of negligible phase-space blocking effects, the equation for the excitonic polarization is equivalent to a modified version of the nonlinear Schrödinger equation, for which soliton solutions have been derived by Mihalache *et al.* [D. Mihalache *et al.*, Phys. Rev. A **47**, 3190 (1993)]. The numerical study demonstrates the solitonlike propagation of experimentally relevant input pulses in CdSe crystal and assesses the influence of phase-space blocking effects and dephasing processes. [S1063-651X(98)00907-6]

PACS number(s): 42.65.Tg, 42.81.Dp, 71.35.Gg

I. INTRODUCTION

The issue of solitonlike light pulse propagation for ultrashort light pulses that propagate in semiconductors and that are spectrally centered in the vicinity of the strongest-bound Wannier exciton has been investigated theoretically from several different perspectives [1–8]. Common to all approaches is the basic idea that optical nonlinearities necessary for the formation of solitons can result from exciton-exciton interactions and excitonic Pauli-blocking effects. As for theoretical investigations, the necessity for approximations leads to differences in the various treatments and differences in the form of the solutions. In addition to the theoretical studies, solitonlike pulse propagation has been recently reported for systems exhibiting certain similarities to Wannier excitons, namely, for light pulses in the spectral region of the biexciton two-photon transition in CuCl [9] and the bound-to-impurity exciton resonance in CdS [10].

Independently of the issues of light pulse propagation (i.e., polariton and/or soliton issues), ultrafast optical nonlinearities of excitons in a direct-gap semiconductor have been studied extensively both theoretically (see, e.g., Refs. [11,12]) and experimentally (see, e.g., Refs. [13,14]). The resulting comprehensive theoretical framework for the description of excitonic optical nonlinearities has been used for detailed investigations of analogies and differences of two-level atoms and excitons in semiconductors. An important aspect linking optical nonlinearities with solitonlike light pulse propagation is the issue of Rabi oscillations. In atomic systems, Rabi oscillations provide the basic processes enabling self-induced transparency (SIT) [15]. Analogous processes in semiconductors have been studied theoretically (see, e.g., Ref. [16]) and experimentally [17]. Other theoretical studies of nonlinear light pulse propagation based on the framework of the semiconductor Bloch equations include, for example, Refs. [5,18].

Because of the advantages of theoretical treatments that result in analytical soliton solutions and the simultaneous problem that certain approximations, which are necessary for finding analytical solutions, may result in oversimplifications, we will present in the following a combined analytical and numerical study of solitonlike [19] pulse propagation. This approach enables us to discuss the soliton phenomena to be expected in idealized semiconductor systems, and, for the same model, to discuss modifications due to dephasing processes. In Sec. II we review briefly the well-established theoretical model and discuss its analytical soliton solutions. We show that the investigations on completely different physical systems [20] lead to soliton solutions that can also be applied to excitons. We discuss the nature of the resonant solitons and also compare them with two well-investigated optical soliton phenomena, namely, the SIT in atomic systems [15,21–23] on the one hand and propagation of femtosecond optical solitons in optical fibres [24] on the other hand. At the same time, we amend the specific shape of the solitary-wave solution given in [8] and consider the case of exact-resonance excitation. In Sec. III we present a numerical investigation of the soliton formation from experimentally relevant nonchirped sech-shaped initial pulses and discuss the influence of dephasing processes. Finally, we discuss the validity of the model and the parameter regimes for possible experimental verification in Sec. IV and summarize the results in Sec. V.

II. THEORETICAL MODEL AND ANALYTICAL SOLUTIONS

The interaction between a light pulse and a semiconductor medium can be described semiclassically by Maxwell's equations together with the semiconductor Bloch equations (MSBE). In the slowly varying envelope approximation, the electric field of the light is given by $\mathcal{E}(z,t) = \frac{1}{2}\tilde{E}(z,t)\exp[i(k_L z-\omega_L t)]$, the material polarization $\mathcal{P}(z,t)=\frac{1}{2}\tilde{P}(z,t)\exp[i(k_L z-\omega_L t)]$, and Maxwell's wave equation can be reduced to the form

$$\frac{\partial\tilde{E}(\xi,\eta)}{\partial\xi} = i\frac{2\pi}{c^2}\frac{\omega_L^2}{k_L}\tilde{P}(\xi,\eta), \tag{1}$$

*Present address: Fachbereich Physik, Philipps-Universität Marburg, 35032 Marburg, Germany.

where ω_L is the optical carrier frequency, k_L is the propagation constant of the light pulse, and $\eta = t - z/U$ and $\xi = z$ are the time and distance in the moving coordinate frame. The velocity of the moving frame, U, is a fictional light velocity in the medium. It takes into account only those transitions that are far off resonant with the pulse carrier frequency. The effect of the transitions in the spectral vicinity of the light pulse is treated explicitly by the equations governing the material polarization. These equations will be discussed in the following.

The interband polarization of direct semiconductors is governed by a set of generalized Bloch equations. Common approximations include the two-band approximation (i.e., one valence band and one conduction band, both with twofold spin degeneracy), and the screened Hartree-Fock approximation [12]. For a recent review of the underlying Green's function techniques see, for example, Ref. [16]. In the following, we employ these approximations and further simplify the theory, thus restricting ourselves to semiconductors with large exciton binding energies such as CuCl, CdS, CdSe, or ZnSe. The advantage of a large exciton binding energy is that an optical pulse centered at the $1s$-exciton resonance can be chosen to be short (and, correspondingly, spectrally broad) without creating higher lying exciton or band-to-band continuum excitations. As a result, excitation-induced dephasing can be kept to a minimum and, furthermore, the pulse duration can be made shorter than the dephasing time of the $1s$-exciton polarization. The semiconductor excitation dynamics within this model have been investigated in detail (see, e.g. [16,25]), but the consequences of this model on the nonlinear propagation dynamics of the light pulse have not been considered.

The reduced semiconductor Bloch equation for the induced polarization of the $1s$ exciton, $P(\xi, \eta)$, reads [12]

$$\frac{\partial P}{\partial \eta} = -i[\delta + \beta_1 |P|^2 - i\gamma_2]P + \frac{i}{2}[1 - \beta_2 |P|^2]\Omega, \quad (2)$$

where $\Omega = d_{cv}\tilde{E}/\hbar$ is the Rabi frequency, d_{cv} is the interband dipole matrix element, $\delta = \omega_{1s} - \omega_L$ is detuning from the exciton resonance, γ_2 is a phenomenological dephasing rate, $\beta_1 = (26/3)\omega_b$ and $\beta_2 = 7$ are the nonlinear exchange and phase-space blocking parameters for the $1s$ exciton [26,27], $\hbar\omega_b$ is the exciton binding energy, and $\tilde{P} = [4d_{cv}/\pi a_0^3]P$ (a_0 is the exciton Bohr radius). The exciton density corresponding to a given value of P is given by $n = 2|P|^2/(\pi a_0^3)$, where the factor of 2 is based on the assumption of a twofold spin degeneracy of the optical transitions.

Before proceeding to an analytical treatment of Eqs. (1) and (2), it is worthwhile to point out the physical aspects of the excitonic nonlinearities in Eq. (2). There are two different physical sources of nonlinearities in our model. The first source is the β_1 term in Eq. (2), which results from noncompensation of the band-gap renormalization and reduction of binding energy in the presence of light field. This noncompensation is in contrast to the almost perfect compensation in quasistationary pump-probe three-dimensional (3D) configurations as shown experimentally, for example, in Ref. [28], and theoretically in Refs. [29–31]. Deviations from this exact compensation have been discussed and observed in the two-dimensional case [32,33]. We want to point out again that Eq. (2) presents only the simplest limiting case of the more general theory, in which the numerical investigation of the ultrafast excitonic shift and bleaching behavior can be done along the lines presented, for example, in Refs. [16,34]. An experimental observation of a blueshift of the exciton peak during passage of the pump pulse, which may be related to the ultrashort single-pulse nonequilibrium dynamics considered in this paper, has been reported in Ref. [35].

The second source of the nonlinearity in Eq. (2) is the β_2 term, which is associated with phase-space blocking effects and has a direct analog in the theory of two-level systems. Although both, the blueshift of the exciton resonance (β_1 term) and phase-space blocking effects (β_2 term) could be responsible for the formation of solitonlike pulses in a semiconductor medium, the first one is more relevant, as we show below and as has already been indicated in Ref. [25]. The set of propagation Eqs. (1) and (2) is closely related to the model equations studied previously in the context of the excitonic SIT [1]. A different aspect of the model used in this paper is that the exchange contributions to the MSBE are analyzed in the low intensity limit (see, e.g., Ref. [16] for details). This leads to a modified (namely, linearized) conservation law relating the carrier density to the $1s$ excitonic polarization $|P|^2$. This modified conservation law prevents the β_2 related (phase-space filling) mechanism from being the actual source of the soliton formation. In other words, the physical course, which leads to the SIT phenomenon in atomic systems is essentially eliminated in our model. To investigate this point in more detail, we present, in the following, an analytical bright soliton solution for the case $\beta_2 = 0$, i.e., for the case where the only nonlinearity is due to exciton-exciton interactions.

We restrict ourselves to the case of zero detuning of the pulse center frequency with respect to the $1s$-exciton resonance ($\delta = 0$). In the following analytical treatment we also neglect dephasing processes ($\gamma_2 = 0$). The soliton solution of Eqs. (1) and (2) is characterized by $P(\xi, \eta) \to P(x)$ where $x = \eta - \xi/V$ (V is the group velocity of the soliton pulse within the moving frame). Thus, the set of MSBE (1) and (2) becomes

$$\dot{P} = -i\beta_1 |P|^2 P + \frac{i}{2}(1 - \beta_2 |P|^2)\Omega, \quad (3a)$$

$$\dot{\Omega} = 2iaVP, \quad (3b)$$

where $a = (4|d_{cv}|^2\omega_L^2)/(\hbar c^2 k_L a_0^3)$ and ''dot'' denotes differentiation with respect to x.

We consider now the case of negligible inversion ($\beta_2 = 0$), i.e., the model where the propagation of the bright soliton pulses is supported entirely by the exchange interaction among the excitons [β_1 term in Eq. (2)]. We show that the pulse propagation in this case has an interesting analogy with femtosecond soliton propagation in optical fibers, and, in particular, with the theory developed in Ref. [20].

For $\beta_2 = 0$, defining $P = P'/\sqrt{\beta_1}$, we obtain the nonlinear excitonic polarization equation

$$\frac{\partial^2 P'}{\partial x^2} + i\frac{\partial(|P'|^2 P')}{\partial x} = aVP'. \tag{4}$$

Formally, Eq. (4) represents a stationary version of the modified nonlinear Schrödinger equation for which analytical solutions have been presented in Refs. [20,36,37]. The nonlinear term in Eq. (4) bears resemblance to the self–steepening effect that arises for femtosecond pulse propagation in nonlinear optical fibers [24]. Using the stationary form of the one-soliton solution derived in Ref. [20], we obtain a bright soliton solution for the excitonic polarization:

$$P'(x) = \sqrt{\frac{2}{x_0}}\sqrt{\mathrm{sech}\left(\frac{x}{x_0}\right)}e^{i\phi(x)}, \tag{5}$$

where $\phi(x) = 3\arctan(e^{-x/x_0})$. Substituting the solution (6) for P' into Eq. (2) and defining $\Omega = \Omega'/\sqrt{\beta_1}$, we obtain the corresponding solution for the electric field as

$$\Omega'(x) = \sqrt{2}x_0^{-3/2}\sqrt{\mathrm{sech}\left(\frac{x}{x_0}\right)} \times \exp\left[i\phi(x) + i\ \arctan\left(\sinh\frac{x}{x_0}\right)\right]. \tag{6}$$

It is interesting that the pulse area for the soliton formation, which can be estimated from Eq. (6), depends on the input pulse duration as $\tau^{-1/2}$ [i.e., the time integral of Eq. (6) and, thus, the pulse area is proportional to $\tau^{-1/2}$].

As mentioned above, in the presence of the β_1 term in Eq. (2) the solution for P and Ω is *always* phase modulated. The corresponding frequency chirp $\dot{\phi}$ is proportional to $\beta_1|P|^2$. Therefore, the solitonlike pulse propagation might be viewed to be analogous to the temporal soliton phenomenon that arises as a result of counterbalance between nonlinear self-phase modulation and dispersion processes.

III. NUMERICAL RESULTS AND DISCUSSION

A. Pulse propagation dynamics

Whereas the model of a spectrally completely isolated exciton resonance seems to be realizable by careful selection of the semiconductor material, the neglect of all dephasing processes is a severe restriction of the theoretical model. Also, in actual experiments it is hardly possible to use input pulses corresponding to the soliton solution given by Eq. (6). Instead, in analogy to excitation of Kerr solitons, one would hope that nonsoliton input pulses evolve automatically into solitonlike pulses during the course of the propagation. In order to discuss these issues, we present in the following the results of a numerical investigation. Equations (1) and (2) are solved using a fourth-order Runge-Kutta method with the initial condition $P(\eta = -\infty) = 0$. The material parameters of bulk CdSe are used ($\hbar\omega_{1s} = 1.8255$ eV, $\omega_b = 24.3$ ps^{-1}, $a_0 = 5.8$ nm, $\epsilon_0 = 9.3$). The input pulse envelope function is chosen to be $\tilde{E}(\eta) = E_0\mathrm{sech}(\eta/\tau_0)$, which is the experimentally relevant case. The input pulse duration is $\tau = 3$ ps [intensity full width at half maximum (FWHM), $\tau = 1.76\tau_0$] and the center frequency of the pulse is chosen to be at the

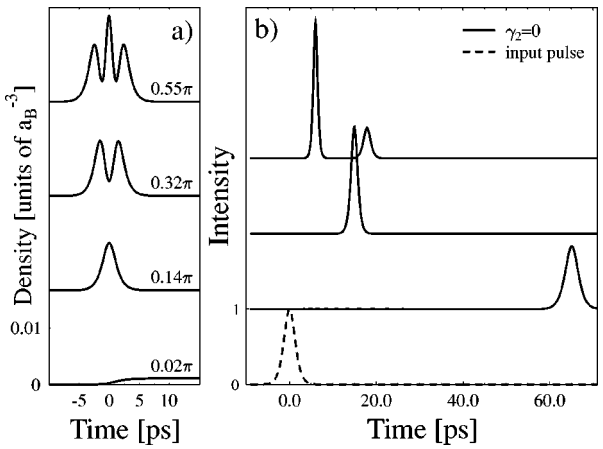

FIG. 1. (a) Computed temporal oscillations in the light-induced charge-carrier density at $z = 0$ for the case of coherent excitation at the A-exciton resonance of a CdSe crystal. The input pulse duration is 3 ps (FWHM), the input pulse area is varied between 0.02π and 0.55π. Results for different pulse areas are shifted vertically for clarity. (b) The temporal intensity profiles after a propagation distance of 0.5 μm for the same excitation conditions as in (a). The transmitted pulse intensities are normalized to the value of the corresponding input intensities.

$1s$-exciton resonance ($\delta = 0$). The input pulse area $A(z = 0)$ is used as variable parameter.

Shown in Fig. 1(a) is the computed light-induced carrier density at $z = 0$ as a function of time (dephasing processes are neglected at this stage, $\gamma_2 = 0$). For weak excitation [$A(z = 0) = 0.02\pi$], a typical absorption behavior is found. When the input pulse area is increased, the carrier density starts to exhibit Rabi-like oscillations [16,25]. The 0.14π pulse yields one complete Rabi-like flop in the carrier density and the 0.32π pulse yields two flops, and so on. Throughout this paper the pulses that yield an integer number of Rabi-like flops in the density are referred to as ''N'' pulses ($N = 1,2,\ldots$). Note that the nature of the observed Rabi-like oscillations in the exciton density is associated with the local optical nonlinearities as discussed in Ref. [25].

We now study the consequences of the Rabi-like oscillations on the propagation dynamics of the light pulses. Numerically, the semiconductor is discretized into slices (10 000 slices per 1 μm of propagation). The optical field calculated from the nonlinear optical response of the first slice [solution of Eq. (1)] serves as an initial condition for the second slice, and so on. Shown in Fig. 1(b) are the temporal intensity profiles of the pulses transmitted through a 0.5 μm thick CdSe crystal for the same excitation conditions as in Fig. 1(a). For weak excitation [$A(z = 0) = 0.02\pi$], we recover the results obtained for propagation of small-area ultrashort light pulses through a resonant medium (anomalous absorption) [38,39]. With an increase in the input pulse area, the most remarkable features observed are an increase in the pulse propagation velocity, the temporal pulse narrowing, and the subsequent pulse breakup.

An intuitive explanation of the pulse velocity dynamics is as follows. Below the threshold for the soliton formation, the only influence of the exciton resonance on the pulse propagation is an absorption at the central pulse frequency. The spectral wings of the pulse remain unaffected by the absorp-

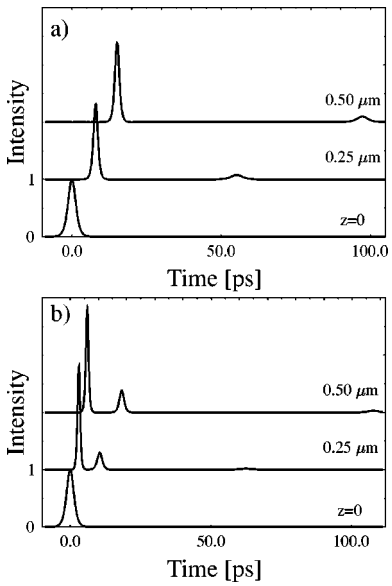

FIG. 2. (a) Computed temporal intensity profiles of the $N=2$ pulse at different propagation distances z. The transmitted pulse intensities are normalized to the value of the corresponding input intensities. (b) The same as in (a) for the $N=3$ pulse.

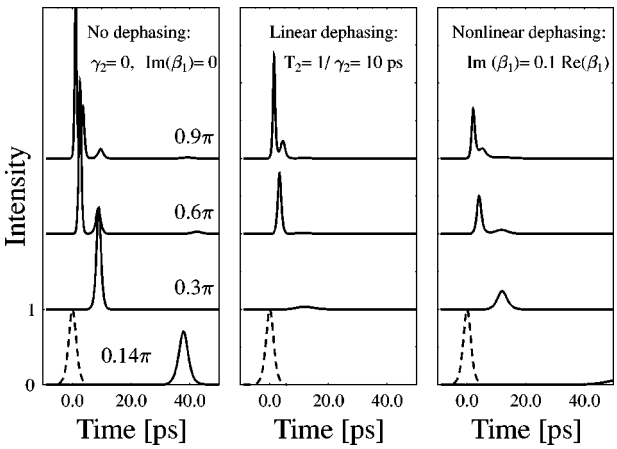

FIG. 3. Computed temporal intensity profiles of the transmitted pulses ($z=0.5$ μm). Results for different input pulse areas are shifted vertically for clarity. Three different cases are shown: no dephasing, $\gamma_2=0$, $\mathrm{Im}(\beta_1)=0$ (left); linear dephasing, $\gamma_2\neq 0$, $\mathrm{Im}(\beta_1)=0$ (central); and intensity-dependent dephasing, $\gamma_2=0$, $\mathrm{Im}(\beta_1)\neq 0$ (right). The transmitted pulse intensities are normalized to the value of the corresponding input intensities.

tion, and their inteference during propagation leads to the frequency beats which are seen in the time domain as oscillations in the pulse envelope (anomalous absorption [39]). The front of this modulated signal travels at the speed close to the light velocity in the medium. Above the threshold for the soliton formation, the nonlinear shift of $1s$-exciton Rydberg energy described by the β_1 term in Eq. (2) effectively detunes the pulse central frequency from the exact exciton resonance. As the initial pulse area increases, the nonlinear shift of the resonance frequency increases as well, and the pulse travels faster through the medium, as it is seen in Fig. 1(b). As for the pulse narrowing, one can see from Eq. (6) that an increase in the (initial) pulse amplitude results in increased soliton amplitude which, in turn, yields a decrease in the soliton duration. The issue of pulse breakup will be discussed in the following subsection.

B. Pulse breakup and influence of dephasing

Figures 1(b) and 2 demonstrate the effect of propagation-induced pulse breakup which takes place for larger-area pulses. For comparison, we also show results for a nonzero dephasing rate in Fig. 3. In Fig. 2(a), the specific features of the pulse breakup are shown for the $N=2$ pulse in the case $\gamma_2=0$: the pulse breaks into two pulses, which have different amplitudes and velocities—the smaller-amplitude pulse moves slower. The $N=3$ pulse in Fig. 2(b) breaks into three pulses during the propagation. An analysis of the effects of dephasing on pulse propagation is presented in Fig. 3, where, for various input intensities, the results without dephasing (left), with linear dephasing, $\gamma_2\neq 0$, (central) and with intensity-dependent dephasing, $\mathrm{Im}(\beta_1)\neq 0$, (right) are plotted. The nonlinear dephasing is introduced by taking a complex value of the nonlinear exchange parameter: $\beta_1=\beta_1^0-\Delta\beta_1$ with $\beta_1^0=(26/3)\omega_b$ and $\Delta\beta_1=0.1\beta_1^0(1+i)$. Such a model, i.e., a reduction of the real part of β_1 and simultaneous occurrence of an imaginary part of β_1 by the same order of magnitude is suggested by the contributions to the semiconductor Bloch equations beyond the Hartree-Fock approximation [see, for example, Eqs. (395)–(396) of Ref. [16]]. While it is difficult to determine the exaxt complex renormalization of β_1 in purely excitonic systems, it is instructive to study the influence of this renormalization on pulse-propagation characteristics with parametric values for $\Delta\beta_1$.

As for the nonlinear dephasing (imaginary part of $\Delta\beta_1$), one can see from Fig. 3 that both linear and nonlinear (intensity-dependent) dephasing processes lead to the same effect on the transmitted pulse profile—they tend to eliminate the pulse breakup features. More parametric dependencies of pulse propagation characteristics on $\Delta\beta_1$ will be discussed below (cf. Fig. 7).

C. Pulse propagation characteristics: pulse area and energy

It is important to emphasize that, in contrast to atomic SIT, the number of pulses into which a given input pulse breaks up during propagation does not only depend on the area of the input pulse, but also on its duration. For example, the specific areas defining the $N=1,2,3$ pulses in Fig. 1 would have been different if we had chosen a different duration of the input pulse. This information can be visualized by representing the excitation conditions that are required to generate N pulses in an A-τ (input pulse area versus input pulse duration) diagram. In Fig. 4, the two lowest-order branches associated with the formation of the $N=1$ and $N=2$ pulses are plotted. Note that, in the case of atomic SIT, the A-τ diagram contains horizontal lines at $A=2\pi$ and 4π for the two lowest-order soliton branches [15,21,22]. In Fig. 4, we compare the $N=1$ numerical branch with the A-τ correlation of the analytical model discussed above, i.e., Eq. (6), which predicts a $\tau^{-1/2}$ dependence of the pulse area. The constant of proportionality between area and duration was obtained from a numerical integration of Eq. (6) and the definition of the effective pulse area [5,40]

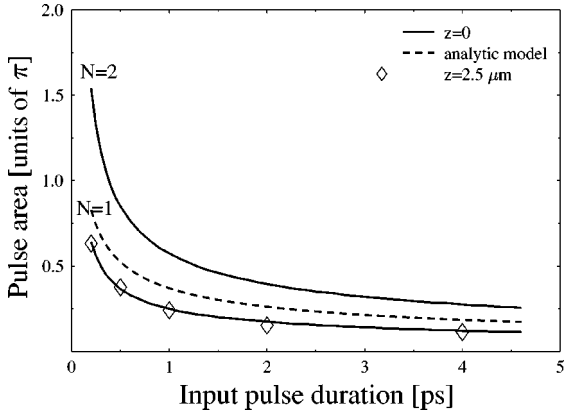

FIG. 4. The A-τ diagram (input pulse area vs input pulse duration) for the two lowest-order branches corresponding to the excitation conditions for formation of the $N=1$ and $N=2$ pulses. The analytical $\tau^{-1/2}$ dependence for the $N=1$ pulse in the case $\beta_2=0$ is shown as dashed line. Note that for atomic SIT the A-τ diagram would contain horizontal lines at $A=2\pi$ and 4π for the two lowest-order soliton branches.

$$A(z)=\left[\left\{\int \mathrm{Re}[\Omega(z,\eta)]d\eta\right\}^2+\left\{\int \mathrm{Im}[\Omega(z,\eta)]d\eta\right\}^2\right]^{1/2}. \tag{7}$$

Good agreement between the analytical ($\beta_2=0$) and the numerical ($\beta_2\neq 0$) A-τ dependence for the $N=1$ pulse indicates that the origin of the A-τ correlation is mainly due to the excitonic exchange interactions (β_1 term).

To further analyze the stability of low-order solitonlike pulses, we show in Fig. 5 the dependence of the pulse area on propagation distance. In the case of the $N=1$ pulse with $A(0)=0.14\pi$, the pulse area is relatively well conserved during propagation. The $N=2$ pulse shows a completely different behavior than the $N=1$ pulse: its pulse area exhibits harmonic oscillations as function of propagation distance. Note that the spatial period of the $A(z)$ oscillations depends on τ: the period increases with decreasing τ. A direct comparison of the area characteristics with the well-known McCall and Hahn area theorem would be possible only in the case of vanishing phase modulation of the pulse, $\mathrm{Im}\,\Omega\rightarrow 0$,

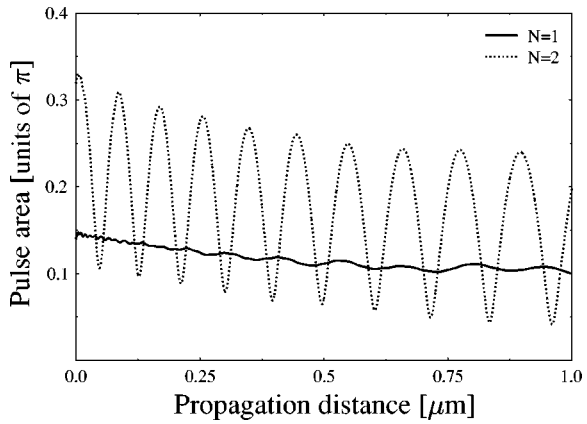

FIG. 5. Effective pulse area $A(z)$ [see Eq. (7)] vs propagation distance for 3 ps pulses with different initial areas. Shown are the $A(z)$ branches corresponding to the $N=1$ [$A(0)=0.14\pi$] and the $N=2$ [$A(0)=0.32\pi$] pulses.

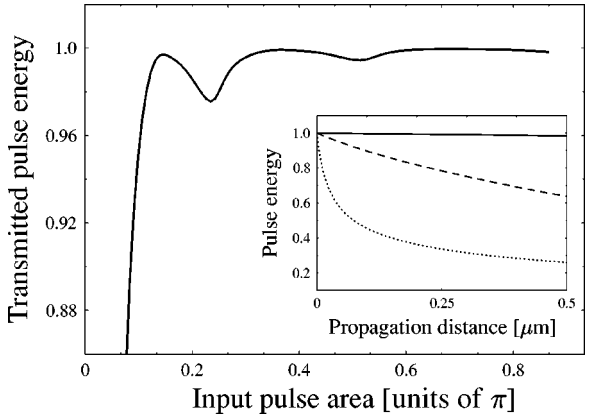

FIG. 6. Computed normalized transmitted pulse energy vs input pulse area for a 3 ps input pulse after a propagation distance of $z=0.25\ \mu$m in the case $\gamma_2=0$. The maxima of the plotted curve correspond to the pulses with $N=1,2,3$. The inset shows the normalized pulse energy vs propagation distance in the cases of the $N=1$ pulse and $\gamma_2=0$ (solid line), the $N=1$ pulse and $\gamma_2=0.05\ \mathrm{ps}^{-1}$ (dashed line), and a weak 0.02π pulse and $\gamma_2=0.05\ \mathrm{ps}^{-1}$ (dotted line).

when Eq. (7) reduces to the usual pulse area definition [15]. A comparison with so-called chirped SIT [40] shows that the pulse area dynamics in our model is clearly different (see also Ref. [41]).

In Fig. 6, we plot the normalized pulse energy

$$W(z)=\frac{c\epsilon_0}{2}\int |\tilde{E}(z,\eta)|^2 d\eta \tag{8}$$

as a function of the input pulse area for the fixed propagation distance of 0.25 μm. The maxima of the plotted curve correspond to the pulses with $N=1$, $N=2$, and $N=3$ ($\gamma_2=0$). The inset in Fig. 6 shows the transmitted pulse energy as a function of propagation distance: the weak pulse (0.02π) is rapidly absorbed during propagation whereas the energy of the $N=1$ pulse remains nearly constant in the case $\gamma_2=0$. A small energy loss for the $N=1$ pulse could be associated with a contribution of the weak anomalous absorption signal that is delocalized in time and cannot be filtered out of the numerical integration. The basic features of the solid curve shown in Fig. 6 resemble typical soliton phenomena [22–24], i.e., the thresholdlike behavior of the transmitted energy at a certain pulse area as well as higher order solutions exhibiting a relative transmitted-pulse energy of values approaching 1.

Finally, we investigate the effect of reduction in the value of the nonlinear parameter β_1 on the soliton dynamics. Figure 7 shows that a decrease in the β_1 value leads to an increase in the area for the $N=1$ soliton formation. This result is quite obvious: the less nonlinearity is attainable from the medium, the more input energy is required to form the soliton pulses.

IV. VALIDITY OF THE MODEL

The range of strict validity of the the analytical model and the solution (6) is restricted to the case of low inversion and, consequently, rather long pulses. More specifically, one can

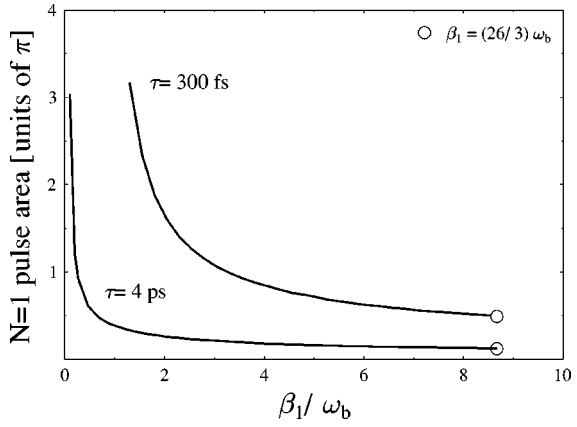

FIG. 7. The A-β_1 diagram (input pulse area vs nonlinear exchange parameter) shows the effect of reduction in the real part of the parameter β_1 on the area of the fundamental soliton ($N=1$). The results for two different input pulse durations are shown for comparison.

estimate from Eq. (6) that, in the case of bulk CdSe with $\omega_b = 24.3\ \mathrm{ps}^{-1}$ (16 meV), if the upper limit for the carrier occupation function is chosen to be 0.1 (generally, it is between 0 and 1), the duration of the soliton is 5.4 ps (FWHM in intensity). The additional condition of negligible linear dephasing (which, in the low excitation regime, is mainly given by the intrinsic dephasing rate) would be fulfilled if the dephasing time is, for example, in the 10 ps regime. While large, this is a realistic value for high-quality samples. In general, one can say that, for a given intrinsic dephasing one should choose the pulse as long as possible (but shorter than the dephasing time), because this avoids complications due to higher-order exciton-exciton interactions and, at the same time, keeps the excitation-induced dephasing to a minimum.

V. SUMMARY

A solitonlike propagation of low-intensity ultrashort light pulses in semiconductors, spectrally centered at the $1s$-exciton resonance, has been studied. An analytical soliton solution of the propagation equations for the electric field amplitude and the induced excitonic polarization has been obtained in the limit of negligible phase-space filling effects. We have discussed the formal similarities between the excitonic solitonlike pulse propagation and a model describing propagation of temporal bright Kerr solitons in the presence of self-steepening effects.

We have demonstrated numerically the formation and propagation of solitary waves for experimentally relevant nonchirped sech-shaped initial pulses. The characteristics of these solitary pulses have been studied in detail and the assumptions underlying the soliton model have been discussed. We have shown that the pulse breakup, predicted by the model, is less pronounced in the presence of linear and excitation-induced dephasing processes. The results may be useful for the understanding of more comprehensive models based on the numerical solution of the Maxwell-semiconductor Bloch equations including many-body effects such as screening and excitation-induced dephasing.

ACKNOWLEDGMENTS

The authors are grateful to E. Wright and M. Lindberg for helpful discussions. We acknowledge major financial support by the U.S. Army Research Office (ARO), and additional support by the Joint Services Optics Program (JSOP) and COEDIP (University of Arizona).

[1] A. Schenzle and H. Haken, Opt. Commun. **6**, 96 (1972); J. Goll and H. Haken, Phys. Rev. A **18**, 2241 (1978).
[2] V. M. Agranovich and V. I. Rupasov, Fiz. Tverd. Tela **18**, 801 (1976) [Sov. Phys. Solid State **18**, 459 (1976)].
[3] O. Akimoto and K. Ikeda, J. Phys. A **10**, 425 (1977).
[4] W. Huhn, Opt. Commun. **57**, 221 (1986).
[5] S. W. Koch, A. Knorr, R. Binder, and M. Lindberg, Phys. Status Solidi B **173**, 177 (1992); A. Knorr, R. Binder, M. Lindberg, and S. W. Koch, Phys. Rev. A **46**, 7179 (1992).
[6] C. R. Stroud, Jr., C. M. Bowden, and L. Allen, Opt. Commun. **67**, 387 (1988); C. M. Bowden, A. Postan, and R. Inguva, J. Opt. Soc. Am. B **8**, 1081 (1991).
[7] I. B. Talanina, M. A. Collins, and V. M. Agranovich, Solid State Commun. **88**, 541 (1993); Phys. Rev. B **49**, R1517 (1994); I. B. Talanina, Solid State Commun. **97**, 273 (1996).
[8] I. B. Talanina, J. Opt. Soc. Am. B **13**, 1308 (1996).
[9] K. Ema and M. Kuwata-Gonokami, Phys. Rev. Lett. **75**, 224 (1995).
[10] M. Jütte, H. Stolz, and W. von der Osten, Phys. Status Solidi B **188**, 327 (1995).
[11] H. Haug and S. Schmitt-Rink, Prog. Quantum Electron. **9**, 3 (1984).
[12] H. Haug and S. W. Koch, *Quantum Theory of the Optical and Electronic Properties of Semiconductors*, 2nd ed. (World Scientific, Singapore, 1993).
[13] S. Schmitt-Rink, D. S. Chemla, and D. A. B. Miller, Adv. Phys. **38**, 89 (1989).
[14] C. F. Klingshirn, *Semiconductor Optics* (Springer-Verlag, Berlin, 1995).
[15] S. L. McCall and E. L. Hahn, Phys. Rev. Lett. **18**, 908 (1967); Phys. Rev. **183**, 457 (1969).
[16] R. Binder and S. W. Koch, Prog. Quantum Electron. **19**, 307 (1995).
[17] S. T. Cundiff, A. Knorr, J. Feldmann, S. W. Koch, E. O. Göbel, and H. Nickel, Phys. Rev. Lett. **73**, 1178 (1994).
[18] W. Schäfer and K. Henneberger, Phys. Status Solidi B **159**, 59 (1990).
[19] Following the usual convention, we make no distinction between the solitary waves that we study and the strict mathematical definition of solitons as elements of the discrete spectrum of the eigenvalue problem within the corresponding inverse scattering transform (if it exists). We refer to both of them as solitons.
[20] D. Mihalache, N. Truta, N.-C. Panoiu, and D.-M. Baboiu, Phys. Rev. A **47**, 3190 (1993).
[21] G. L. Lamb, Jr., Rev. Mod. Phys. **43**, 99 (1971).

[22] L. Allen and J. H. Eberly, *Optical Resonance and Two-Level Atoms* (Wiley and Sons, New York, 1975).
[23] H. M. Gibbs and R. E. Slusher, Phys. Rev. Lett. **24**, 638 (1970).
[24] G. P. Agrawal, *Nonlinear Fiber Optics* (Academic Press, Boston, 1989).
[25] A. Knorr, Th. Östreich, K. Schönhammer, R. Binder, and S. W. Koch, Phys. Rev. B **49**, 14 024 (1994).
[26] L. V. Keldysh and A. N. Kozlov, Zh. Éksp. Teor. Fiz. **54**, 978 (1968) [Sov. Phys. JETP **27**, 521 (1968)].
[27] Th. Östreich and A. Knorr, Phys. Rev. B **50**, 5717 (1994).
[28] G. W. Fehrenbach, W. Schäfer, J. Treusch, and R. G. Ulbrich, Phys. Rev. Lett. **49**, 1281 (1982).
[29] R. Zimmermann, K. Kilimann, W. D. Kraeft, D. Kremp, and G. Röpke, Phys. Status Solidi B **90**, 175 (1978).
[30] *Optical Nonlinearities and Instabilities in Semiconductors*, edited by H. Haug (Academic Press, New York, 1988).
[31] W. Schäfer, K. H. Schuldt, and R. Binder, Z. Phys. B **70**, 145 (1988).
[32] N. Peyghambarian, H. M. Gibbs, J. L. Jewell, A. Antonetti, A. Migus, D. Hulin, and A. Mysyrowicz, Phys. Rev. Lett. **53**, 2433 (1984).
[33] D. R. Wake, H. W. Yoon, J. P. Wolfe, and H. Morkoc, Phys. Rev. B **46**, 13 452 (1992).
[34] S. Hughes, A. Knorr, S. W. Koch, R. Binder, R. Indik, and J. V. Moloney, Solid State Commun. **100**, 555 (1996).
[35] P. C. Becker, D. Lee, M. R. X. de Barros, A. M. Johnson, A. G. Prosser, R. D. Feldman, R. F. Austin, and R. E. Behringer, IEEE J. Quantum Electron. **28**, 2535 (1992).
[36] D. J. Kaup and A. C. Newell, J. Math. Phys. **19**, 798 (1978).
[37] A. S. Rodrigues, M. Santagiustina, and E. M. Wright, Phys. Rev. A **52**, 3231 (1995).
[38] D. C. Burnham and R. Y. Chiao, Phys. Rev. **188**, 667 (1969).
[39] M. D. Crisp, Phys. Rev. A **1**, 1604 (1970).
[40] L. Matulic and J. H. Eberly, Phys. Rev. A **6**, 822 (1972); L. Matulic *et al.*, J. Opt. Soc. Am. B **8**, 1276 (1991).
[41] I. Talanina, R. Binder, D. Burak, N. Peyghambarian, and H. Giessen, in *Quantum Electronics and Laser Science Conference*, 1997 OSA Technical Digest Series Vol. 12 (Optical Society of America, Washington, D.C., 1997), p. 192.